On the Adiabatic Motion of Energetic Particles in a Model Magnetosphere

JUAN G. ROEDERER[1]

Goddard Space Flight Center, Greenbelt, Maryland

The motion of charged particles in a model magnetosphere is studied using the three adiabatic invariants. The particle shell geometry is determined, and drift velocities, bounce periods, and equatorial pitch angles are computed as a function of local time. The following conclusions were reached: (1) Shell splitting in the outer magnetosphere becomes important beyond 5 R_E (earth radii). This means that particles mirroring at different points on the *same* field line at noon appear *spread* over a region of field lines at midnight, and vice versa. (2) There are regions in the magnetosphere, where only pseudo-trapped particles can mirror, i.e. particles that will leave the magnetosphere before completing a 180° drift. (3) Longitudinal drift velocities depart considerably from the dipole values beyond 5 R_E, and can be as much as 2–3 times greater on the night side than on the day side. Thus a given particle spends 2–3 times more time in the day side than in the night side. (4) After recovery from a prototype magnetic storm, particles that were in the day side during the sudden commencement will have higher energies, their shells having moved radially inward. Particles caught in the night side will have moved outward, with their energies decreased.

1. INTRODUCTION

Recent experimental results on trapped particle flux behavior in the outer magnetosphere indicate that physical processes governing particle diffusion and acceleration are strongly influenced by the trapping field itself and by the time changes of its configuration. The main evidence comes from the observed strong correlations between particle flux and energy spectra variations beyond 2–3 R_E (earth radii), with geomagnetic perturbations such as the sudden commencement of a geomagnetic storm or the ring current during the main phase [*Frank*, 1966; *McIlwain*, 1965; *McIlwain*, 1966]. It seems therefore useful to attempt a detailed theoretical description of the behavior of a flux of trapped particles using a reasonably accurate magnetospheric field model, and simulating prototype time variations of the field configuration. The first detailed studies of this type were done by *Hones* [1963] for auroral particles, and by *Fairfield* [1964] for energetic particles.

There are several sources of the field in the geomagnetic cavity: the magnetization of the earth's interior, the currents flowing on the surface of the magnetopause, the currents in the 'neutral sheet' of the tail of the magnetosphere, and, eventually, diamagnetic ring currents originating in trapped particle density gradients at 2–4 R_E. At geocentric distances of less than, say, 4 R_E, the internal geomagnetic field dominates; beyond 4 R_E, the currents in the magnetopause (and in the neutral sheet) perturb the dipole-type internal field and introduce a strong noon-midnight asymmetry. Any model must take these sources into account.

Before adopting de facto a given field model, let us list our requirements. First, we are mainly interested in particles trapped on field lines reaching out beyond, say, 5 R_E, on the equatorial plane. This means that we can safely ignore all higher multipoles of the internal field and replace it by a centered dipole. Second, we shall also ignore the effect of a ring current. Third, we shall consider the dipole axis perpendicular to the sun-earth line, which of course is a very substantial limitation. However, a 'wobbling' dipole would make our calculations immensely more complicated, without, however, adding much to the general results, at least within the scope of this paper. Finally, electric fields will be ignored; this

[1] National Academy of Sciences—National Research Council, Senior Post Doctoral Research Associate. Present address: Centro Nacional de Radiacion Cosmica, Rivadavia 1917, Buenos Aires, Argentina.

means that we are restricting ourselves to particles of high enough energy to ensure that the gradient drift always prevails over the *EB* drift.

A model that satisfies these requirements and has already predicted or explained experimental results with good quantitative agreement is that given by Mead [*Mead*, 1964; *Williams* and *Mead*, 1965; *Mead*, 1966]. This model considers two sources, in addition to the internal dipole; currents in the magnetopause, and currents in the tail of the magnetosphere. Four adjustable parameters determine the field in Mead's model: (1) the distance R_0 from the center of the earth to the magnetopause, in the solar direction; (2) and (3), the distances R_{min}, R_{max} from the center of the earth to the close and far limit, respectively, of the neutral sheet in the antisolar direction, respectively; and (4) the field intensity B_T near the neutral sheet. Most of the typical planetary variations of the geomagnetic field can be simulated by appropriate variations of these parameters. See section 4 for choice of parameters actually used.

Figure 1 shows field lines of this model in the noon-midnight meridian, corresponding to the parameters we shall adopt as describing the quiet-time state of the magnetosphere.

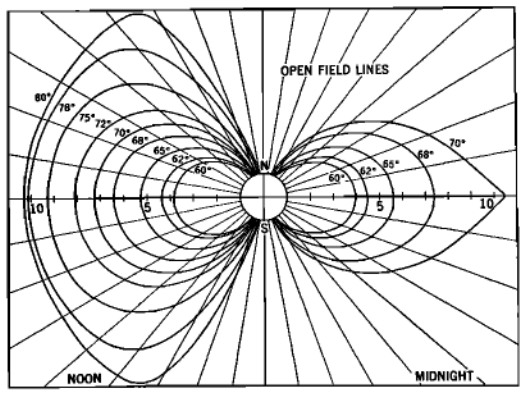

Fig. 1. Closed field lines in the model magnetosphere, for parameter values given in the text. Field lines are labeled with the geomagnetic latitude of their intersection with the earth's surface.

2. Adiabatic Invariants

The motion of charged particles in a trapping field geometry can be described by means of three adiabatic constants of motion [*Northrop*, 1963], the magnetic moment M, the second invariant J, and the flux invariant Φ:

$$M = p_\perp^2/2m_0B \tag{1}$$

$$J = \oint p_\parallel \, ds \tag{2}$$

$$\Phi = \oint \mathbf{A}\cdot d\mathbf{x} \tag{3}$$

In these equations $p_\perp$ and $p_\parallel$ are components of the momentum perpendicular and parallel to the magnetic field vector, respectively; B is the magnetic field intensity at the instantaneous position of the guiding center; and m_0 is the rest mass. In (2) the integration is extended along the field line for a complete bounce oscillation; ds is the element of arc of the field line. Equation 3 represents the magnetic flux enclosed by the particle shell; **A** is the magnetic vector potential, and the integral is extended along any closed path passing around the particle shell and lying in it. These quantities are adiabatic constants, i.e. conserved only under certain conditions. Adiabaticity requires that the field configuration should not change appreciably during the characteristic period of time associated to each invariant. If this condition is violated, the corresponding value of the invariant will no longer be conserved. The other two may still remain unaffected.

In place of (1) and (2) we shall introduce two other expressions that are much more convenient for numerical computations. According to (1), we introduce the mirror point field intensity B_m:

$$B_m = p^2/2m_0M \tag{4}$$

where p is the total momentum of the particle. Further, we introduce the geometric integral

$$I = \int \left(1 - \frac{B(s)}{B_m}\right)^{1/2} ds = \frac{J}{2p} \tag{5}$$

extended along the field line between one mirror point and its conjugate. B_m and I uniquely determine a particle shell and will be used in what follows as the two identifying parameters for such a shell. Notice at once that for a time-independent magnetic field, in absence of electric fields, (4) and (5) are adiabatic invari-

ants, too. The advantage of (4) and (5) is that they only depend on the field geometry. For time-dependent fields, care has to be taken regarding relation 5. If p changes appreciably during one bounce, we have:

$$\frac{J}{2\bar{p}} = \frac{1}{2\bar{p}} \oint p(s)\left(1 - \frac{B(s)}{B_m}\right)^{1/2} ds \neq I \qquad (5')$$

Equation 5 holds at all times only for slowly varying fields.

Introducing the usual relativistic factor $\gamma = m/m_0$, we can combine (4) and (5) with (1) and (2) to obtain

$$(\gamma^2 - 1)I^2 = K_1 = \text{const} \qquad (6)$$

$$I^2 B_m = K_2 = \text{const} \qquad (7)$$

To these, we must add (3), which we write in the form:

$$\Phi = \Phi(B_m, I) = K_3 = \text{const} \qquad (8)$$

These are the adiabatic constants that will be used henceforth. They uniquely determine γ, I, and B_m for any static field configuration. For time-dependent fields, K_1 and K_2 in general are not constant *during* the interval of change [see (5')]. However, if this interval is transient, i.e. if it is preceded and followed by time-independent states of the field, the constancy of K_1 and K_2 *does* hold when (6) and (7) are evaluated for the initial and the final states.

For a field constant in time, (8) is no longer needed, and γ, I, and B_m are conserved individually. A special case is that of particles mirroring on or close to the equator ($I = 0$, $B_m = B_e$). In that case we replace (6) by the following, derived from (4):

$$\frac{1}{\gamma^2 - 1} B_e = \text{const} \qquad (6a)$$

This holds all the time, even in nonstatic fields. In this special case, (8) is a function of B_e only.

We have to add Liouville's theorem to relations 6, 7, and 8 to complete our description of trapped particle dynamics. We introduce the directional, differential flux of particles populating a given I, B_m shell:

$$j = j(\gamma, I, B_m)$$

$$\text{cm}^{-2} \times \text{sec}^{-1} \times \text{ster}^{-1} \times \text{kev}^{-1} \qquad (9)$$

Consider particles of given (I, B_m) in a steady-state distribution on a given shell. For each point of the shell, there is a unique cone along whose elements the given group of particles is streaming. This direction is the particles' pitch angle, which at the equatorial points of the shell is given by

$$\alpha_e = \arcsin (B_e/B_m)^{1/2} \qquad (10)$$

where $B_e = B_e(I, B_m;$ azimuth) is the minimum or equatorial B value of a particular field line of the shell. We must point out at once that even for time-independent fields, α_e is *not* an adiabatic invariant like the mirror point field B_m; in general it will depend on azimuth (longitude or local time) through B_e.

The particle density in phase space f associated with the flux (9) is given by $f = j/p^2$. Liouville's theorem states that this density in phase space remains constant along the dynamical path of a particle. This means that, as long as all particles always remain on a common shell (this condition will be fulfilled if all invariants (6)–(8) are conserved throughout the evolution of the system), even if the shell itself changes with time, the following conservation theorem holds:

$$\frac{j(\gamma, I, B_m)}{\gamma^2 - 1} = K_4 = \text{const} \qquad (11)$$

(6), (7), (8), and (11) are the basic expressions to be used for the study of the evolution in space and time of trapped particles in the outer magnetosphere. The first three lead to the determination of the actual shell of a given group of particles and their actual energy; equation 11 gives the actual value of the directional differential flux of this group of particles.

As was shown by *Newkirk and Walt* [1964], the average equatorial azimuthal drift velocity u of the particles populating an I, B_m shell can be obtained as a direct consequence of Liouville's theorem. The value is, with our notation:

$$u = \frac{m_0 c^2}{eB_e} \frac{\gamma^2 - 1}{\gamma} \frac{\nabla I}{S_b} \qquad (12)$$

∇I is the limit of $\delta I/\delta y$ where δy is the equatorial distance between two neighboring shells, each one characterized by I and $I + \delta I$, re-

spectively, and by the same B_m value. S_b is the half-bounce path, i.e. the rectified path of the particle between one mirror point and its conjugate:

$$S_b = \int \left(1 - \frac{B(s)}{B_m}\right)^{-1/2} ds$$

S_b is related to the bounce period by $\tau_b = 2S_b/v$ where v = particle velocity. We can obtain an expression for S_b by taking the derivative of (5) with respect to the mirror point field intensity B_m along a given field line. It can be shown by simple algebra that

$$S_b = I + 2B_m \frac{\partial I}{\partial B_m} \tag{13}$$

The derivative has to be taken along the given field line. This expression has general validity for any trapping field geometry and is very useful for computational purposes, for it only requires the calculation of I on two neighboring points of a field line.

3. Qualitative Discussion

Before getting into the discussion of numerical computations for particle shell geometry and time variations of the model magnetosphere, it is useful to present a qualitative analysis of the consequences of the previous section. First, let us envisage a trapping magnetic field constant in time. In this case, (4) and (5) are conserved. We can assign to each point in space a pair of values I, B_m such that a particle mirroring *there* has the value I for the integral (5), B_m being simply the field intensity at that point. In this way, I and B_m become uniform functions of space. As the particle drifts to other field lines, it must keep these values constant; i.e., it will cover a shell of field lines that pass through the intersections of two given constant-I and constant-B_m surfaces (Figure 2). Notice carefully that the surface I = const is *not* the particle shell.

Let us consider the geomagnetic field. Take a particle that starts at a given longitude Φ, circling around a given field line and mirroring at a value B_m. The integral (5) computed along the field line between the two mirror points has a value I. This means that when drifting through any other longitude, say 180° away, this particle will be bouncing along a

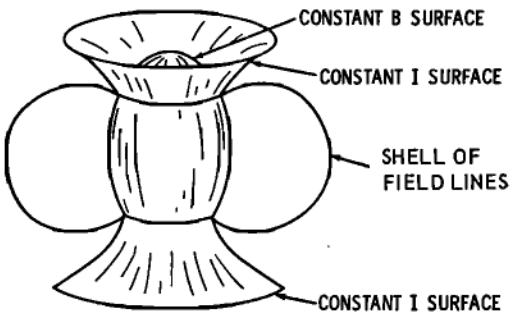

Fig. 2. Geometric definition of a particle shell.

field line that passes through the intersection of the corresponding I = const and B_m = const surfaces. Now take a particle that starts on the *same* initial field line but mirrors at a lower value $B'_m < B_m$ (Figure 3). Its integral (5) will also be smaller, $I' < I$. After a 180° longitudinal drift, this second particle will be traveling along a field line that passes through the intersection of the surface I' = const and B'_m = const. *Only* in case of perfect azimuthal symmetry (as in the pure dipole) will these surfaces intersect exactly on the *same* line as that of the first particle. In the general case, particles starting on the same field line at a given longitude will populate different shells, according to their initial mirror point fields, or, what is equivalent, according to their initial equatorial pitch angles (10) (of course, all these different shells would be tangent to each other at the initial field line) [*Stone*, 1963].

For the case of the real geomagnetic field in absence of external perturbations, i.e. within about 3–4 R_E, it can be shown that the distance between split shells is relatively small, a fraction of 1% of the distance of the equatorial point of a field line to the center of the

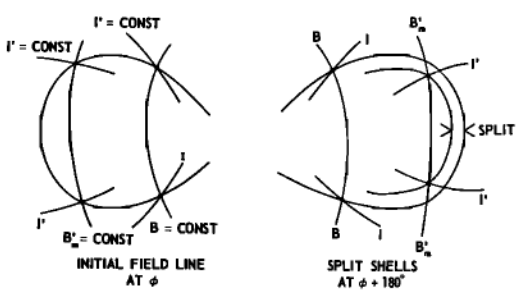

Fig. 3. Shell splitting in asymmetric fields.

earth. In other words, with a very good approximation, one can say that *all* particles initially on the same field line will mirror on a common field line at any other longitude. This has an important consequence: it enables a two-dimensional description of the three-dimensional radiation belts, at least up to distances of about 4 R_E. Indeed, if particles do populate the same shell irrespective of their initial mirror points, the omnidirectional flux of these particles will be the same on all points of the shell having the same B value, irrespective of the longitude, i.e. local time, (provided, of course, no appreciable injections or losses occur during the drift). To describe omnidirectional particle fluxes in the inner magnetosphere, we therefore need only two 'space' parameters: the value of the magnetic field intensity at the point of measurement and a parameter that characterizes the (unique) shell that goes through that point. This latter is McIlwain's L parameter [*McIlwain*, 1961]. L is a particular relation between I and B_m that remains constant (within $\lesssim 1\%$) on a given field line and, therefore, on the whole shell generated by particles starting on that field line. Numerically, L gives the average distance of the equatorial points of a shell to the magnetic center.

But what happens in the outer magnetosphere, where the azimuthal symmetry is brutally removed? Particles starting on the same field line, say in the noon meridional plane, will now populate different shells, depending on their initial mirror points or equatorial pitch angles. For instance, they will cross the midnight meridian on *different* lines.

Let us start with a particle mirroring at or near the equator, on a line in the noon meridian, close to the boundary. For this particle, $I \simeq 0$; according to (6*a*) it will drift around the earth on the equator following a constant-B path. This constant-B path comes considerably closer to the earth at the night side, because the field is weaker there (less compression), and we must go to lower altitudes to find a given B value. On the other hand, a particle that starts on the same field line on the noon meridian, but is mirroring at high latitudes, will have a high I value. Under these circumstances, *Mead* [1966] has shown that the value of I is not much different from the

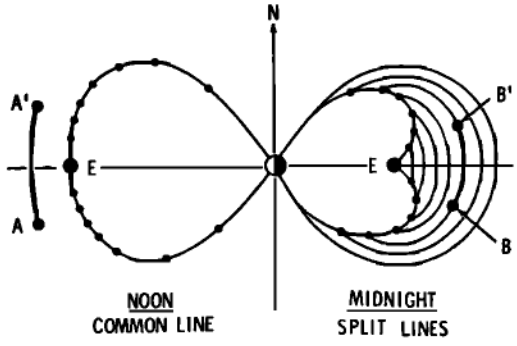

Fig. 4. Qualitative picture of shell splitting in a model magnetosphere for particles starting on a common field line in the noon meridian.

arc length of the field line between mirror points. On the midnight meridian, the particle will therefore be found on a line having nearly the same length as the initial one, i.e. stretching out to roughly the same equatorial distance. In summary, all particles initially on the same noon line, will cross the midnight plane on line portions sketched in Figure 4. Furthermore, it is easy to realize that particles mirroring inside that area (BB') will cross the noon meridian outside (AA') of the initial line. If this noon line is very close to the boundary, *no* stably trapped particle could be found mirroring inside the hatched area in the midnight meridional plane. Any particle doing this would not be able to complete a drift around the earth: it would abandon the magnetosphere before reaching the noon meridian. We shall call this a *pseudo-trapped* particle (only transiently trapped) [*Roederer*, 1966]. Notice finally that a sharp trapping boundary in the noon side would *not* result in a sharp boundary in the back side.

On the other hand, for a given field line in the midnight meridian, all particles mirroring anywhere on this line will cross the noon meridian in an area like the one shown in Figure 5. All particles mirroring outside that area (BB') will cross the midnight-meridian outside (AA') of the given line. If now there is an 'obstacle' behind that line (like, for instance, the neutral sheet), no stably trapped particle could be found outside the hatched area in the noon meridian. Any particle injected there would be lost into the obstacle before reaching the midnight meridian: in this high-latitude

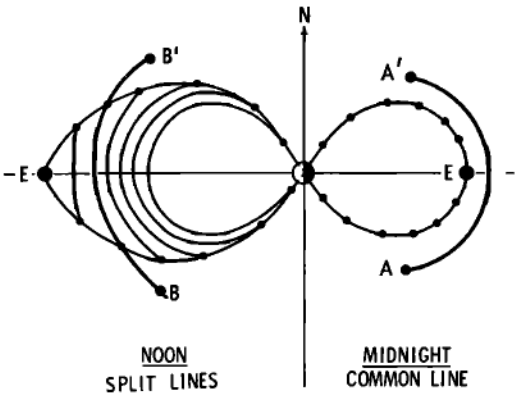

Fig. 5. Qualitative picture of shell splitting for particles starting on a common line in the midnight meridian.

noon region, only pseudo-trapped particles could exist.

4. Numerical Results

A computer code was set up to determine particle shells in the model magnetosphere to study shell splitting and longitude dependence of drift velocities and equatorial pitch angles for the static case and to analyze the evolution of a system of particle shells in a time-dependent case.

This program was applied using Mead's model of the magnetosphere. The numerical values of the four adjustable parameters (section 1) for the quiet magnetosphere were taken from *Ness and Williams* [1966]: $R_s = 10\ R_E$, $R_{min} = 8\ R_E$, $R_{max} = 200\ R_E$, and $B_T = 15\ \gamma$. Typical closed field lines are shown in Figure 1. The kink of the field lines reaching out beyond 8 R_E in the night side is caused by the assumption in Mead's model of a two-dimensional neutral sheet (recent measurements, however, suggest a finite thickness of several earth radii [*Bame et al.*, 1966]). Figure 6 shows the relationship between geomagnetic latitude of the intersection of a field line with the earth's surface and the radial distance to its equatorial point for the noon, midnight, and dawn/dusk meridians.

The code was applied to this quiet-time field configuration to obtain magnetic shells for particles initially mirroring on a common field line and having equatorial pitch angles with cosines 0.2, 0.4, 0.6, 0.8, and nearly 1 (mirroring close to the earth's surface). Figure 7 shows how particles, starting on a common line in the noon meridian, do indeed drift on different shells, which intersect the midnight meridian along the field lines shown in the figure. The dots represent particles' mirror points. Curves giving the position of mirror points for constant equatorial pitch angles are traced for comparison (in a dipole field, they are constant latitude lines). Notice the change (decrease) in equatorial pitch angle for the same particle when it drifts from noon to midnight. Figure 7 clearly confirms our qualitative predictions given in section 2: shell splitting becomes considerable beyond 5 R_E and completely invalidates the use of 'L values' or any other dipole-type description of the outer radiation belt. Figure 8 depicts the same features for particles

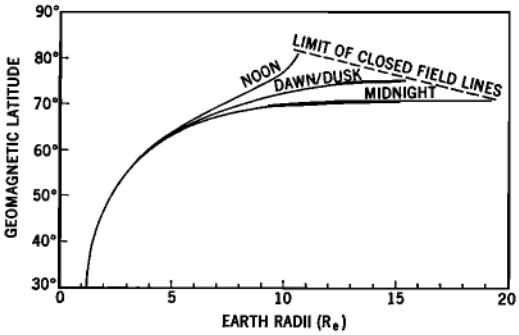

Fig. 6. Relationship between geomagnetic latitude of the intersection of a field line with the earth's surface and the radial distance to its equatorial point, for the noon, midnight, and dawn/dusk meridians.

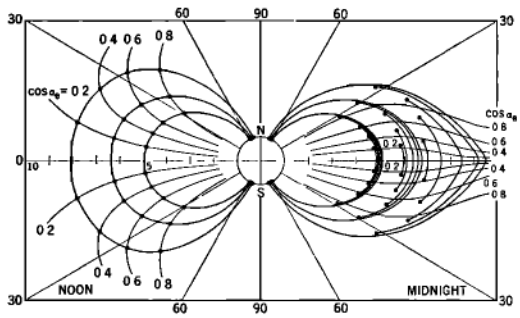

Fig. 7. Computed shell splitting for particles starting on common field lines in the noon meridian. Dots represent particles' mirror points. Curves giving the position of mirror points for constant equatorial pitch angle α_s are shown.

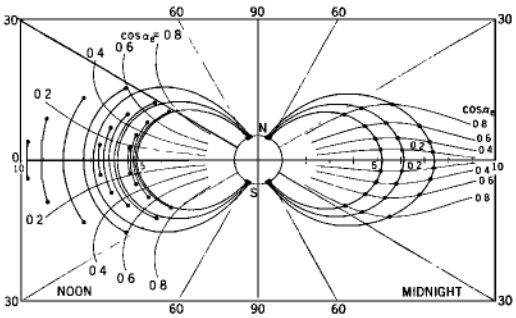

Fig. 8. Computed shell splitting for particles starting on common field lines in the midnight meridian. Dots represent particles' mirror points. Curves giving the position of mirror points for constant equatorial pitch angle α_e are shown.

starting on a common field line in the midnight meridian. In this case, again, the pitch angle changes considerably when the particle drifts to the opposite meridian (increasing at noon).

Notice from Figures 7 and 8 that as equatorial pitch angles increase, shell splitting is directed radially inward for particles starting on the same field line at noon and radially outward for particles starting on a common field line at midnight. Furthermore, shell splitting is maximum for particles mirroring close to the equator: for a given change in pitch angle (in degrees), the radial displacement of the shell will be greater for equatorial particles.

When the initial field line has its equatorial point beyond about 8 R_E, a fraction of the particles mirroring on it can only be pseudo-trapped, being lost before completing a 180° drift. In particular, the computations reveal that particles mirroring at low latitudes in the *back* side abandon the model magnetosphere through the boundary 30–40° before reaching the noon meridian. On the other hand, particles mirroring at high latitudes on the *day* side, run into the tail (open field lines) 10–20° before reaching the midnight meridian. Figure 9 shows computed limits between stable trapping and pseudo-trapping regions on the noon-midnight plane. At other local times, both regions approach more closely the boundary; going from noon to midnight, one disappears at the expense of the growth of the other. These results indicate the existence of a quite considerable loss cone in the day side of the model magnetosphere.

Figures 10*a* and *b* summarize the information about the shell splitting effect. In both figures, the relation between noon and midnight radial distances to the equatorial points of a particle shell is given. In Figure 10*a*, particles start on a common field line at noon, reaching out to R_{noon} earth radii; in Figure 10*b*, particles start on a line at midnight, reaching out to R_{midn}. Curves are labeled with the cosines of the initial pitch angles. Figures 11*a* and *b* show how these pitch angles change when the particles drift to the opposite meridian. Notice again the marked tendency of particles to align along field lines on the night side, and to 'squeeze' transverse to the field on the day side. This is physically explained by the fact that for a given particle shell, the equatorial B value appearing in (10) always decreases toward the midnight meridian, except for particles mirroring close to the equator.

The numerical calculations reveal a considerable local-time dependence of the equatorial drift velocity. The geometrical factors appear-

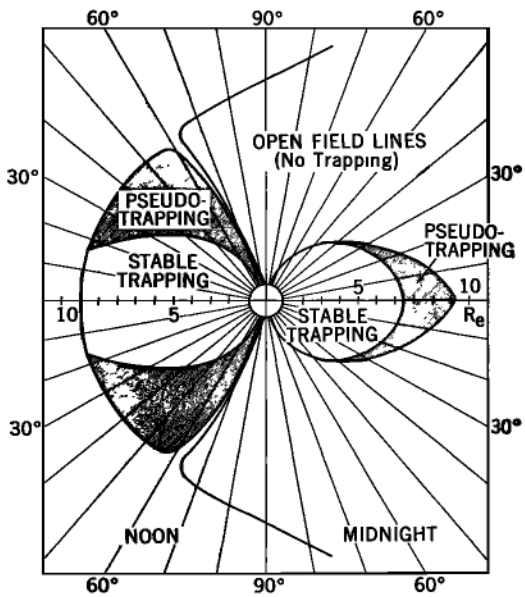

Fig. 9. Location of the 'pseudo-trapping' regions in the magnetosphere. Particles mirroring inside those regions are unable to complete a 180° drift around the earth. Those injected into the left side will be lost into the tail; those injected into the right portion will abandon the magnetosphere through the boundary, on the day side.

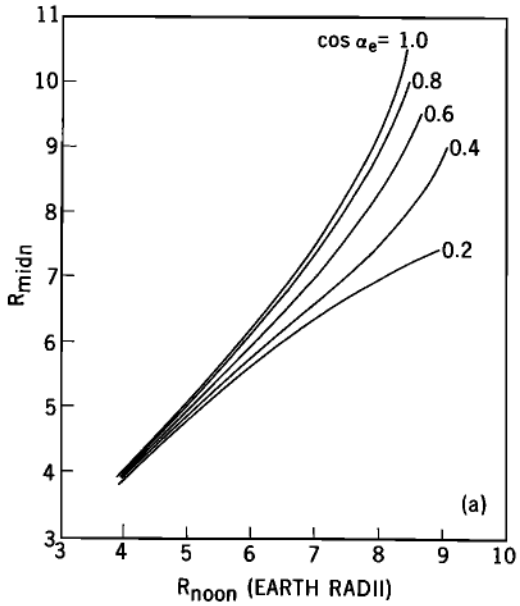

Fig. 10*a*. Particles starting in the noon meridian at a field line reaching out to R_{noon} will cross the midnight meridian on a field line reaching out to R_{midn}. Curves are labeled by the cosine of the particles' equatorial pitch angles.

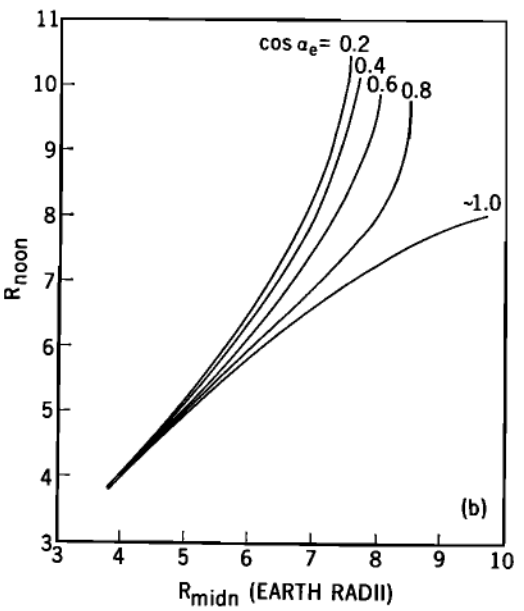

Fig. 10*b*. Particles starting in the midnight meridian at a field line reaching out to R_{midn} will cross the noon meridian on a field line reaching out to R_{noon}.

ing in (12) were computed and represented in Figures 12*a* and *b* as a function of the equatorial distance of the corresponding field line, for different pitch angles, and for noon and midnight, respectively. For a better understanding, *angular* drift factors are shown. For radial distances $<3\ R_E$, we observe a dipole-like dependence. Beyond 3 R_E, there is a considerable departure. Drift velocities on the night side are indeed appreciably higher than on the day side. The peculiar inversion of the pitch-angle dependence, occurring on the day side (Figure 12*a*), is due to a shift in relative importance of curvature drift versus gradient

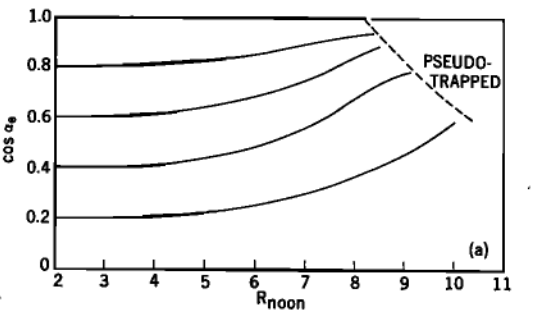

Fig. 11*a*. Particles starting in the noon meridian at a field line reaching out to R_{noon} and initially having equatorial pitch angles of cosines 0.2, 0.4, 0.6, 0.8, and 1.0, respectively, will appear on the midnight meridian with cosines of pitch angles given by the curves. Notice the effect of alignment along the field lines (occurring at midnight), for radial distances $\gtrsim 6$.

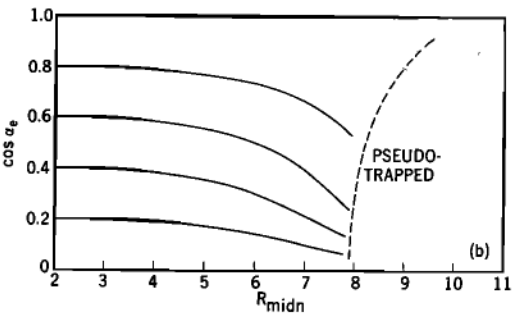

Fig. 11*b*. Particles starting in the midnight meridian at a field line reaching out to R_{midn} and initially having equatorial pitch angles of cosines 0.2, 0.4, 0.6, 0.8, and 1.0, respectively, will appear on the midnight meridian with cosines of pitch angles given by the curves. Notice the effect of alignment along the field lines (occurring at midnight), for radial distances $\gtrsim 5$.

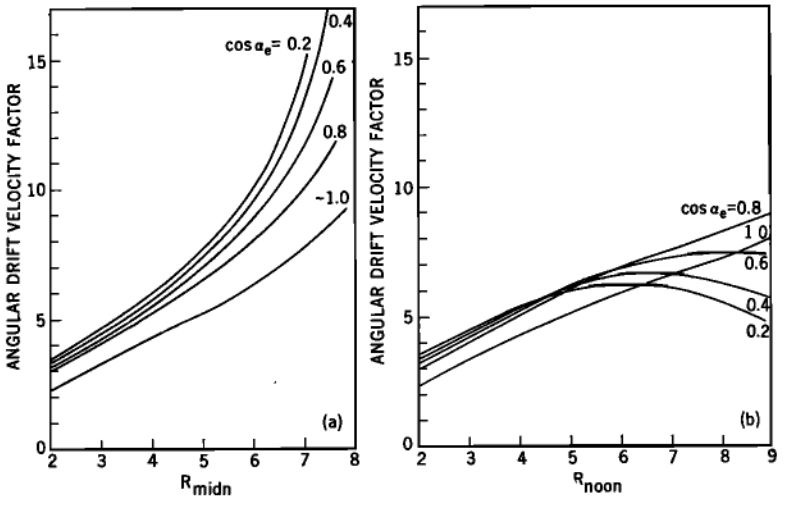

Fig. 12. Value of the geometric factors intervening in the angular drift velocity, as a function of the equatorial distance of the corresponding field line, for different pitch angles, and for noon (*a*) and midnight (*b*), respectively. To obtain drift velocities in degrees/sec, multiply the above values by the factor 2.321×10^{-2} $(\gamma^2-1)/\gamma \times$ (rest mass in electron masses).

drift (particles mirroring at high-latitude experience more of a dipole-type field and drift faster).

In Figures 13*a* and *b* we have represented the percentage change of the linear drift velocity of a given particle, when it drifts to the opposite meridian. A close inspection of the local-time dependence of the drift velocity (not shown here) leads to the important conclusion that a given particle trapped in the outer magnetosphere ($\gtrsim 6\ R_E$) spends up to ⅔–¾ of its total lifetime in the day side. In other words, there is always a higher probability to find a particle in the day side than in the night side. It can be shown that, as a consequence, particle volume densities can be about two times greater on the moon meridian, than at midnight, for a given class of particles. This represents an additional important asymmetry for trapped particle fluxes in the outer model magnetosphere.

Any pitch-angle scattering mechanism will lead to radial diffusion, owing to shell splitting: inspection of Figures 4 and 5 reveals that, for instance, a scattering process that, occurring on the noon side, increases the pitch angle (lowers B_m) will bring the particle to a shell that on the average gets closer to the earth. The same scattering process, occurring on the night side, would situate the particle on a shell extending further out. *Any* type of pitch-angle diffusion process will therefore be accompanied by a radial diffusion, which will be inward or outward according to *where* in longitude the particles are more likely caught by the individual processes. If the original pitch-angle scattering process is elastic, there would be *no* change in energy in this type of radial diffusion. Such a diffusion mechanism was experimentally observed in the laboratory and studied theoretically, by *Gibson et al.* [1963]. According to the preceding results, this radial diffusion will be most effective for equatorial particles. This mechanism would tend to mix and blur energy spectra of particles at different radial distances. Furthermore, the existence of large pseudo-trapping regions, especially on the day side, implies an efficient particle sink for any pitch-angle scattering mechanism (enhanced loss cone). On the other hand, the reverse could also be true: particles that happened to enter the pseudo-trapping regions from outside, could be scattered into stably trapped orbits by any pitch-angle scattering mechanism.

We now turn to the numerical results for a time-dependent magnetic field configuration. The purpose is to study the trapped particle

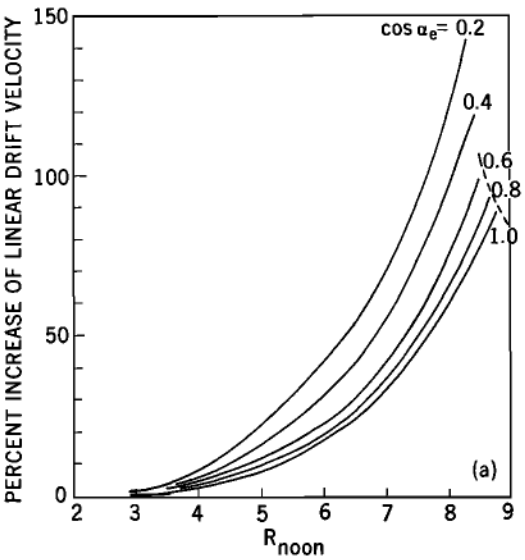

Fig. 13*a*. Maximum percentage increase of the linear drift velocity for particles starting at noon on field lines reaching out to R_{noon} when they drift to the midnight meridian.

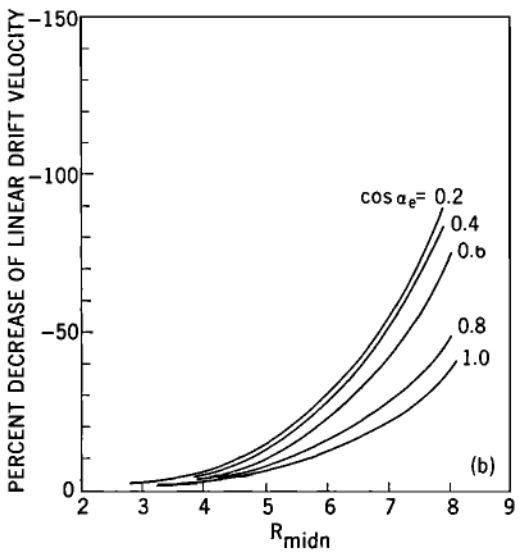

Fig. 13*b*. Maximum percentage decrease of linear drift velocity for particles starting at midnight on a field line reaching out to R_{midn} when they drift to the noon meridian.

behavior during a simulated magnetic storm. The following steps were adopted as a 'model' storm: (1) sudden, nonadiabatic compression, simulated by a decrease ΔR_s of the parameter R_s (inward displacement of the magnetopause); (2) optional sudden increase ΔB_T of the tail field; (3) gradual, adiabatic recovery to the initial field configuration. For (1) and (2) it is assumed that particles, while violating the third invariant (8), stick to their original field line driven by the dominating $E \times B$ drift, still conserving the first two invariants (this 'original' field line is supposed to be rigidly rooted in the ionosphere, during the sudden compression). The gradual recovery in (3) is assumed to be flux-conserving. Some of the results are summarized in Figure 14, in which the percentage change of kinetic energy of a particle is represented as a function of equatorial distance of the initial field line, for different pitch angles, and for particles caught by the compression at noon (upper curves) and at midnight (lower curves). This energy variation is independent of the initial energy and increases with the amount of compression ΔR_s ($\Delta R_s = 2\ R_E$ for the curves in Figure 14). An inward motion of the boundary of only 1 R_E would yield energy changes roughly 0.45 times those shown in the figure. The curves given in Figure 14 were derived for a sudden commencement *without* a sudden increase of the tail field. If one adds a typical increase ΔB_T of 15 γ, acceleration, deceleration, and radial displacements become greater by a factor of about 2, the effect be-

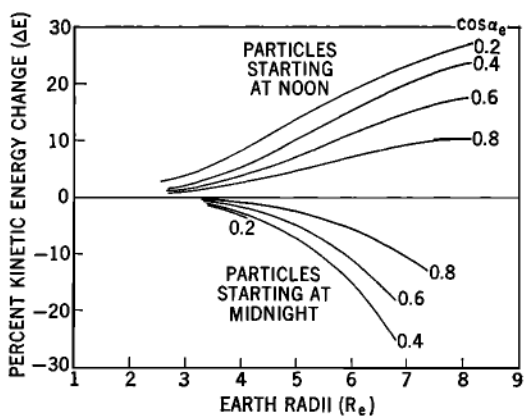

Fig. 14. Percentage kinetic energy change after a prototype storm, for particles caught by the sudden commencement in the noon meridian, and at midnight, respectively, as a function of the radial distance to the equatorial point of the initial field line and for different initial pitch angles. The inward displacement of the boundary was taken as $\Delta R_s = 2\ R_E$.

ing considerably enhanced for particles that were in the night side during the sudden commencement.

One clearly sees in Figure 14 that the final effect of a storm depends on *where* in local time the particle was caught during the nonadiabatic phase: particles that happened to be in the day side of the magnetosphere will have a higher energy when the field recovers to the initial state; particles surprised in the night side will be decelerated. Furthermore, the first group of particles will have moved radially inward, whereas the second group will be found on shells 'inflated' outward (Figure 15). It should be pointed out that during the first phase of compression, *both* groups of particles attain higher energies; it is during the adiabatic recovery that this peculiar asymmetry arises. The fact that a given particle always spends more time in the day side leads to the conclusion that a magnetic storm should always have a *net* effect of inward diffusion and acceleration of trapped particles, after the field has recovered to the same initial configuration. We finally must mention that during a magnetic storm a considerable fraction of particles can be driven into pseudo-trapping regions of the magnetosphere and therefore be lost through the boundary or into the tail. This effect is particularly important for storms with increases of the tail field, which mainly lead to losses through the boundary on the day side. Likewise, particles that for some reason happened to be injected into pseudo-trapping regions during recovery, can become stably trapped, under favorable circumstances of injection.

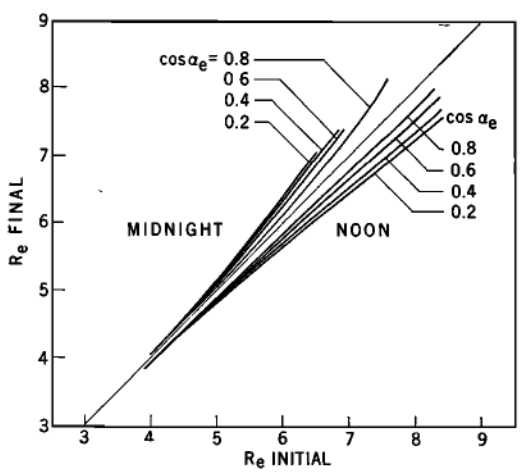

Fig. 15. Relation between initial and final position of the equatorial point of a shell at a given meridian (noon and midnight), after a prototype storm, for particles caught by the sudden commencement at noon and at midnight, respectively ($\Delta R_s = 2$).

The repeated action of magnetic storms will therefore cause acceleration and radial diffusion toward lower altitudes of particles trapped in the outer magnetosphere. This mechanism leads to energy spectra that depend on radial distance, hardening toward lower R values. This is indeed observed for protons [*Davis and Williamson*, 1963; *Vernov et al.*, 1966] and was explained theoretically by *Nakada et al.* [1965]. Electrons, however, should, in addition, be subject to pitch-angle scattering by electromagnetic waves; as discussed above, the radial diffusion that accompanies pitch-angle scattering when shell splitting is considerable should greatly blur the radial dependence of energy spectra for electrons.

5. Conclusions

1. Shell splitting in the outer magnetosphere becomes important beyond 5 R_E; dipole-type descriptions of the radiation belt become invalid.

2. Equatorial pitch angles tend to align along field lines on the night side of the magnetosphere and perpendicularly to the field on the day side.

3. There are regions in the magnetosphere where only pseudo-trapped particles can mirror, i.e. particles that will leave the magnetosphere before completing a 180° drift.

4. Longitudinal drift velocities depart considerably from the dipole values beyond 5 R_E, and they can be as much as 2–3 times greater on the night side than on the day side. Thus a given particle spends 2–3 times more time in the day side than in the night side.

5. The action of a pitch-angle scattering mechanism will lead to a radial diffusion of particles. The loss mechanism will be greatly enhanced by scattering of mirror points into the pseudo-trapping regions.

6. After recovery from a prototype magnetic storm, particles that were in the day side during the sudden commencement will have higher energies, their shells having moved

radially inward. Particles caught in the night side will have moved outward, with their energies decreased.

7. The repeated action of magnetic storms will result in a net inward diffusion of particles, with a net increase of their energy.

Acknowledgments. The author is grateful to Drs. G. Mead, W. N. Hess, and T. Northrop for enlightening discussions. Dr. G. Mead kindly furnished his code for magnetic field computations.

References

Bame, S. J., J. R. Asbridge, H. E. Felthauser, R. A. Olson, and I. B. Strong, Electrons in the plasma sheet of the earth's magnetic tail, *Phys. Rev. Letters, 16,* 138–142, 1966.

Davis, L. R., and J. M. Williamson, Low energy trapped protons, *Space Res., 3,* 365–375, 1963.

Fairfield, D. H., Trapped particles in a distorted dipole field, *J. Geophys. Res., 69,* 3919–3926, 1964.

Frank, L. A., Explorer 12 observations of the temporal variations of low energy electron intensities in the outer radiation zone during geomagnetic storms, *J. Geophys. Res., 71,* 4631–4639, 1966.

Gibson, G., W. C. Jordan, and E. J. Lauer, Particle behavior in a static, asymmetric, magnetic mirror geometry, *Phys. Fluids, 6,* 133–141, 1963.

Hones, E. W., Jr., Motion of charged particles trapped in the earth's magnetosphere, *J. Geo-Phys. Res., 68,* 1209–1219, 1963.

McIlwain, C. E., Redistribution of trapped protons during a magnetic storm, *Space Res., 5,* 347–391, 1965.

McIlwain, C. E., Ring current effects on trapped particles, *J. Geophys. Res., 71,* 3623–3628, 1966.

McIlwain, C. E., Coordinates for mapping the distribution of magnetically trapped particles, *J. Geophys. Res., 66,* 3681–3691, 1961.

Mead, G. D., Deformation of the geomagnetic field by the solar wind, *J. Geophys. Res., 69,* 1181–1195, 1964.

Mead, G. D., The motion of trapped particles in a distorted magnetosphere, in *Radiation Trapped in the Earth's Magnetic Field, Proc. Advan. Study Inst., Bergen, Norway, August 1965,* edited by B. M. McCormac, pp. 481–490, D. Reidel Publishing Company, Dordrecht-Holland, 1966.

Nakada, M. P., J. W. Dungey, and W. N. Hess, On the origin of outer-belt protons, 1, *J. Geophys. Res. 70,* 3529–3532, 1965.

Ness, N. F., and D. J. Williams, Correlated magnetic tail and radiation belt observations, *J. Geophys. Res., 71,* 322–325, 1966.

Newkirk, L. L., and Martin Walt, Longitudinal drift velocity of geomagnetically trapped particles, *J. Geophys. Res., 69,* 1759–1763, 1964.

Northrop, T. G., *The Adiabatic Motion of Charged Particles,* John Wiley & Sons (Interscience) New York, 1963.

Roederer, J. G., Magnetospheric phenomena, in *Proc. Intern. Conf. Cosmic Rays, 9th, London, 1965,* vol. 1, pp. 586–593, The Institute of Physics and the Physical Society, London, 1966.

Stone, E. C., The physical significance and application *of* L, B_0, and R_0 to geomagnetically trapped particles, *J. Geophys. Res., 68,* 4157–4166, 1963.

Vernov, S. N., P. V. Vakulov, S. N. Kuznetsov, Yu. I. Logatchev, A. G. Nikolaev, E. N. Sosnovets, and V G. Stolpovsky, The structure of the earth's radiation belts according to the data of the 'electron' series of satellites, *Space Res., 7,* 1966.

Williams, D. J., and G. D. Mead, Nightside magnetosphere configuration as obtained from trapped electrons at 1100 kilometers, *J. Geophys. Res., 70,* 3017–3029, 1965.

(Received July 6, 1966;
revised September 30, 1966.)